

# The effect of poly(vinyl chloride) blends on the mechanical properties of highly plasticized membranes

M. A. Simon† and R. P. Kusy†‡\*

†Department of Biomedical Engineering, and ‡Department of Orthodontics, University of North Carolina, Chapel Hill, NC 27599-7455, USA

(Received 27 July 1993; revised 15 January 1994)

Solvent polymeric ion-selective electrode membranes are composed primarily of 33% polymer and 66% plasticizer. Puncture tests were conducted on membranes that incorporated blends of poly(vinyl chloride)s (PVCs), fractionated and whole, with different molecular-weight distributions. The extent to which the minor membrane component determines eight modified mechanical properties, i.e. four *elastic* parameters (elastic limit, tangent stiffness, resilience, flexibility) and four *failure* parameters (strength, secant stiffness, toughness, ductility), was investigated. The mechanical properties of fractionated and whole blends were not substantially different. Membrane ductility was always independent of thickness. Elastic parameters showed no effect of polymer number-average molecular weight,  $\bar{M}_n$ . Two of the failure parameters, however, showed a linear blending relationship based on the blend  $\bar{M}_n$ . From that relationship, the per mer contributions of PVC to the membrane strength/thickness and toughness/thickness equalled  $0.96 \text{ mg } \mu\text{m}^{-1}$  and  $0.78 \text{ mg mm } \mu\text{m}^{-1}$ , respectively.

(Keywords: poly(vinyl chloride) blends; plasticized membranes; mechanical properties)

## INTRODUCTION

Poly(vinyl chloride) (PVC), which serves as the support polymer in solvent polymeric electrodes, has allowed the development of many types of ion-selective electrodes (ISEs) based on the liquid ion-exchanger and neutral carrier ionophore sensor<sup>1</sup>. In commercial applications, PVC is plasticized with low-boiling esters in the range of 20–70 phr (per hundred resin). In ISE membranes, the proportion of plasticizer to polymer is 2:1, or 200 phr. This high level is necessary for the plasticizer to facilitate transport of ionophore and ion-ionophore complexes through the membrane. Optimal response times are assured if the membrane is barrier-free and closely approximates a liquid interface.

The cleanliness and purity of the constituents that compose the biosensor membrane are critical. To purify the PVC, residue from the polymerization reaction must be removed along with other added impurities, such as impact modifiers or heat stabilizers<sup>2</sup>. Fractionation of the polymer by high-performance gel permeation chromatography (h.p.g.p.c.) achieves this by recovering the PVC, without the lower-molecular-weight additives and impurities. In addition, the entire molecular-weight distribution (*MWD*) can be partitioned by h.p.g.p.c. into any number of fractions, each with a different *MWD* and material properties.

In such highly plasticized membranes, the relatively small amount of polymer present must be optimized for

overall strength, puncture resistance and processibility. Typically, the physical properties of a polymer degrade rapidly when the plasticizer content increases beyond 40 phr<sup>3</sup>. The *MWD* of a polymer is the single best parameter to define its physical and processing properties<sup>4</sup>; even subtle differences in the *MWD* can dramatically change processing characteristics<sup>5</sup>. By mixing polymers of differing *MWD*s, polymer blends may be designed that exhibit improved material properties such as strength, impact toughness and puncture resistance, without sacrificing the processibility of the material<sup>6–10</sup>.

The current application can be viewed as a reverse single-phase solution, in which the polymer that is usually the major additive now comprises the minority of the membrane. The current study focuses on discovering to what degree the mechanical properties are determined by this now minor membrane component and how the membrane properties can be influenced by appropriate choices of polymer blends. By blending two fractionated and two whole polymers to customize the material properties, a fuller understanding of the structure-property relationships in highly plasticized membrane systems is obtained. Finally, using the average chain length of molecules, a model is employed to predict the strength and toughness of membranes that are plasticized with 200 phr dioctyl sebacate (DOS).

## MATERIALS AND METHODS

### Materials

Blends were made from two standard PVCs of high ('A') and low ('B') molecular weights and from fractions

\* To whom correspondence should be addressed, at: Dental Research Center, CB# 7455, University of North Carolina, Chapel Hill, NC 27599, USA

0032-3861/94/18/3966-12

© 1994 Butterworth-Heinemann Ltd

**Table 1** Molecular-weight characterization of polymers and plasticizer

Material	Code	$\bar{M}_n$ ( $\times 10^{-3}$ )	$\bar{M}_w$ ( $\times 10^{-3}$ )	PDI	Manufacturer <sup>a</sup>
Polymer					
Whole PVC	A	106	198	1.9	SPP
	B	51	94	1.9	SPP
	OXY 410	116	206	1.8	OCC
Fractionated PVC	F1	228	431	2.0	All
	F2	151	222	1.5	fractions
	F3	114	174	1.5	derived
	F4	69	118	1.7	from
	F5	41	76	1.9	OXY 140
Plasticizer					
Diethyl sebacate <sup>b</sup>	DOS	0.520	0.525	1.0	Ald

<sup>a</sup>SPP, Scientific Polymer Products Inc., Ontario, NY; OCC, Occidental Chemical Corp., Pottstown, PA; Ald, Aldrich Chemical Co., Milwaukee, WI

<sup>b</sup>Details of this molecular-weight distribution may be found in figure 4 and table 3 of ref. 20. A trace of dimer is present as well as a higher-order, but as yet unidentified, constituent

('F2' and 'F5') of a commercial PVC, OXY 410 (cf. Table 1). PVC is chosen for its ability to accept the large amounts of plasticizer that are necessary to construct membrane-type ISEs. PVC generally yields membranes of good mechanical stability, electromotive properties and chemical stability<sup>11</sup>. As the lifetime of solvent polymeric membrane electrodes is also mainly governed by the loss of membrane components<sup>12,13</sup>, PVC extends microelectrode life by hindering this process. All samples were plasticized with unmodified dioctyl sebacate (DOS), a relatively pure plasticizer that is commonly used in the design of ISEs<sup>13</sup>.

#### Characterization

All materials were initially characterized via h.p.g.p.c. (model 590, Waters Assoc., Milford, MA) under the following conditions: flow rate, 1.0 ml min<sup>-1</sup>; injection volume, 50  $\mu$ l; sample concentration,  $2.5 \times 10^{-3}$  g ml<sup>-1</sup> maximum; and solvent, tetrahydrofuran (THF). The polymers were analysed with a Waters Ultrastaygel<sup>R</sup> linear analytical column, which was calibrated with 10 polystyrene (PS) standards (Shodex<sup>R</sup>, Showa Denko K.K., Tokyo) ranging in  $\bar{M}_w$  from  $1.32 \times 10^3$  to  $3.03 \times 10^6$ . A g.p.c. calibration curve was derived by using the universal calibration procedure that adapts the Mark-Houwink equations for PS in THF and PVC in THF<sup>14</sup>. The plasticizer was analysed with a Shodex K-Series g.p.c. column specialized for low-molecular-weight organic samples. Calibration was performed with a series of seven low-molecular-weight PS oligomer standards, ranging in  $\bar{M}_w$  from 517 to 3270. Each value of  $\bar{M}_n$ ,  $\bar{M}_w$  and polydispersity index (PDI) represented the average of three sample runs (cf. Table 1).

#### Fractionation

From one commercial polymer, OXY 410, five fractions were collected by h.p.g.p.c. The g.p.c. column was 122 cm in length with a 20 mm i.d. and was packed with  $10^5$  Å Styragel<sup>R</sup> (35–62  $\mu$ m particle size). Run conditions were: flow rate, 9.8 ml min<sup>-1</sup>; injection volume, 3.75 ml; sample concentration, 1% g ml<sup>-1</sup>; and solvent, THF.

Prior to fractionation, the solution of whole polymer was heated to 80°C in a vacuum oven to enhance chain

unfolding<sup>15,16</sup>, cooled to room temperature, and filtered through a 10  $\mu$ m Teflon filter. After fractionation, the polymer was recovered by vacuum distillation in a Buchi evaporator. Fraction solutions were reduced to approximately 10% of original volume and precipitated in 10 times their volume of a non-solvent, methanol. The recovered precipitate was washed with excess methanol and finally dried to constant weight in a 40°C vacuum oven.

#### Membrane preparation

Stock solutions of whole polymers A and B or of fractionated polymers F2 and F5 were prepared at concentrations of 1.1 wt% in THF. PVCs with a  $\bar{M}_w$  greater than 100000 were heated in THF solution in a 85°C vacuum oven for 4 h to enhance solubility<sup>15,16</sup>. The solutions were stirred rapidly overnight. From the stock solutions of A and B or F2 and F5, three blends were prepared with each polymer composing 25%, 50% and 75% of the total volume. To 50 ml of each blend and each stock solution, 1.097 ml of plasticizer was added; the clear solutions were again stirred rapidly overnight.

In the membrane casting technique<sup>17</sup>, glass rings (i.d. = 3 cm) that had ground and polished ends were placed on a glass plate, and 3 to 5 ml of membrane solutions were added. To obtain uniform membrane thicknesses, the evaporation of THF was controlled for a period of 96 h by dead-weighting a stack of filter paper on top of the rings. The resulting membranes had a uniform, not mottled, coloration indicative of a single-phase solution.

#### Mechanical properties

Cast membranes were individually mounted on 0.5 cm sections of Tygon tubing (i.d. = 1.6 cm) by a PVC/THF glue. To relax stress concentrations in the tubing and return it to its original as-manufactured circular cross-section, the tubing was heated for 2 min with a hot-air gun. Tubing sections were machined on a lathe, by using a copper pipe as the spindle and a razor as the cutting tool. Handwheels allowed exact and reproducible placement of the razor, providing sections with square cut surfaces. Prior to testing, all mounted membranes were hydrated for 24 h in a pH 7 buffer solution to

simulate actual use conditions of membranes functioning as ISEs. By using an Instron Universal Testing Machine (Instron Corp., Canton, MA) equipped with a bullet-shaped 0.32 cm metal probe and a specially designed apparatus (Figure 1), sample membranes were punctured at a crosshead speed of 1.0 cm min<sup>-1</sup>, and their force-deflection curves were recorded. Each sample was

tested immediately after its removal from the buffer solution.

After completion of testing, the membranes were sectioned in half with a razor to allow membrane thickness measurements to be made with a Sloan Dektek 3030 profilometer (Santa Barbara, CA). The lightest stylus weight (1.0 mg) was used for a 1.6 mm scan length, which included the membrane edge.

Each membrane puncture test produced a force-deflection curve similar to the one depicted in Figures 2 and 3. These figures also illustrate the modified definitions of the eight mechanical properties that were measured from the curves. The first four mechanical properties are called *failure parameters*, and the second four are *elastic parameters*. The failure parameters were defined by the terminus of the plastic zone of the force-deflection trace<sup>18</sup>: strength, secant stiffness, toughness and ductility (Figure 2). 'Strength' was determined by the maximum force on the force-deflection trace; 'secant stiffness' was indicated by the force at failure divided by the deflection at failure; 'toughness' was determined by the area under the force-deflection trace; and 'ductility' was represented as the maximum deflection at maximum force. The elastic

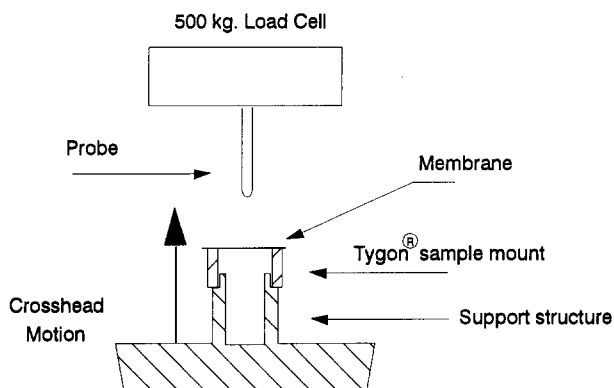


Figure 1 Schematic of the membrane puncture apparatus

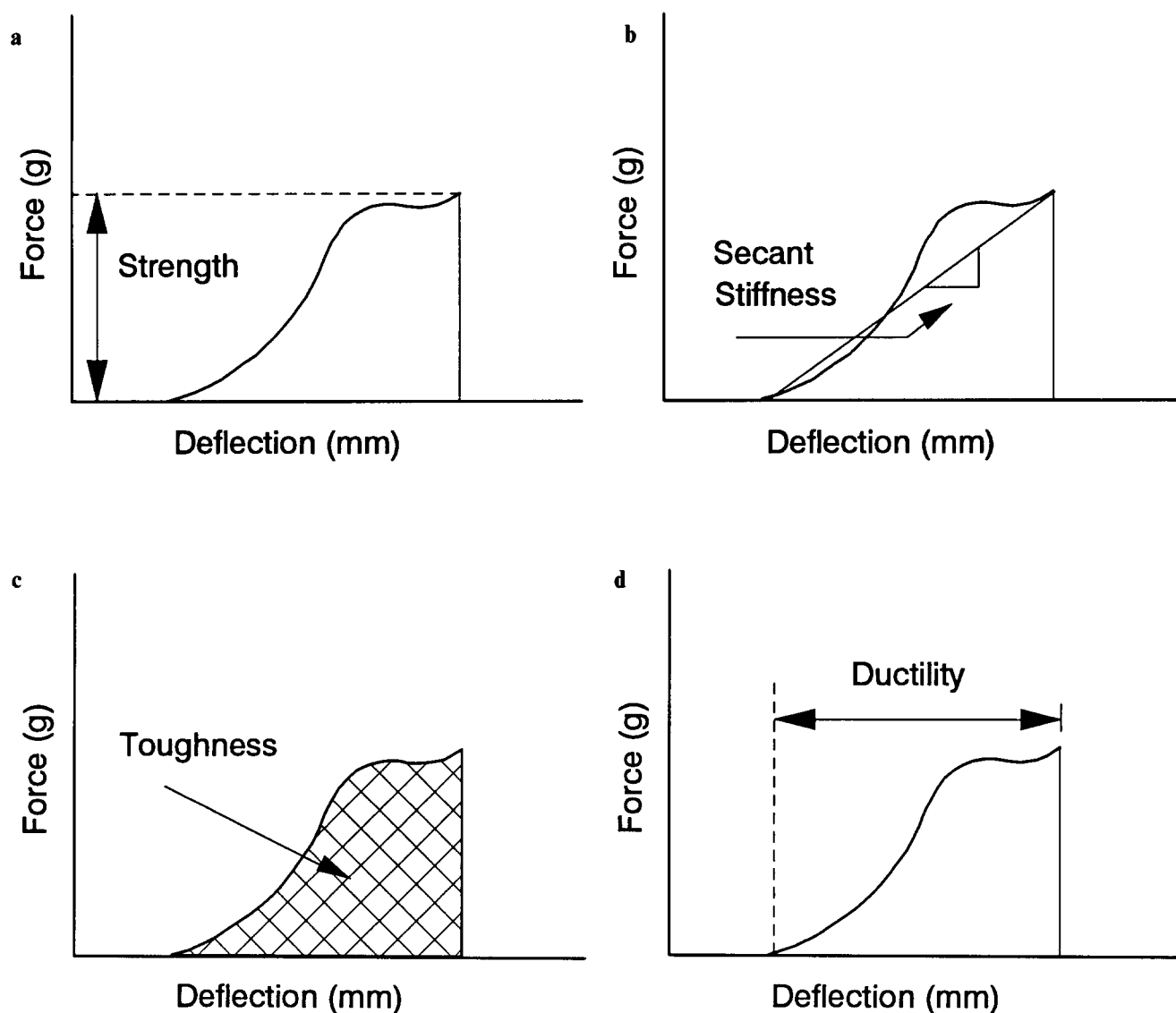


Figure 2 Typical force-deflection trace with the definitions of the four *failure parameters* illustrated

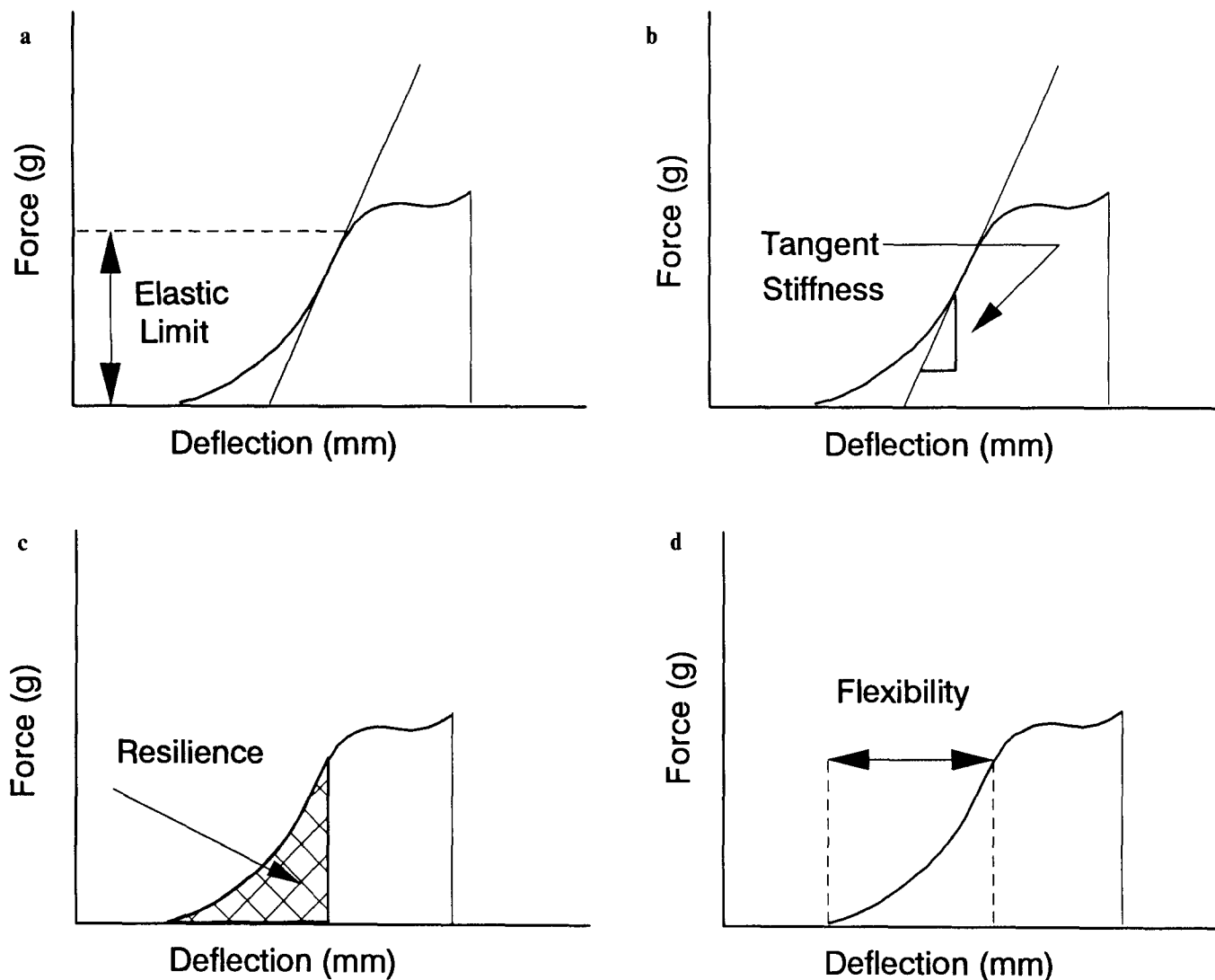


Figure 3 Typical force-deflection trace with the definitions of the four elastic parameters illustrated

parameters were defined by the terminus of the elastic zone of the force-deflection trace<sup>19</sup>: 'elastic limit', 'tangent stiffness', 'resilience' and 'flexibility' (Figure 3). The 'elastic limit' was determined by the force at which a line drawn tangent to the first major upward swing of the curve diverges<sup>19</sup>; 'tangent stiffness' was indicated by the slope of that tangent line; 'resilience' was determined by the area under the force-deflection trace up to the elastic limit; and 'flexibility' was represented as the deflection up to the elastic limit.

#### Statistics

All mechanical properties were linearly regressed against membrane thickness. Slopes ( $m$ ) and correlation coefficients ( $r$ ) were obtained. From the  $r$  values and the number of samples ( $n$ ), the statistical probability ( $p$ ) that the slope differed significantly from zero was established (either  $p < 0.001$ ,  $p \leq 0.01$ , or not significant).

In order to determine outlying samples, first a mean parameter/thickness value and its standard deviation (for each parameter at each blend condition) were calculated from all available data. A membrane sample that had at least three mechanical parameter values (out of a possible eight – four elastic and four failure parameters) that exceeded  $\pm 2SD$  (two standard deviations) of their means was identified as an outlying sample. The points were

encircled and displayed with the results, but were not included in any subsequent data analysis.

## RESULTS

### Characterization

Initial characterization of whole and fractionated polymers (Table 1) showed all  $PDI \leq 2.0$ . A g.p.c. chromatogram shows the relative distribution of the fractionated polymers and its whole polymer (Figure 4). Molecular-weight characterization of DOS, which is adapted from previous work<sup>20</sup>, indicated a  $PDI = 1.0$  despite the fact that there was a trace of dimer and a higher-order, but as yet unidentified, constituent (Table 1).

### Mechanical properties

**Failure parameters.** The failure parameters of whole PVC blends are regressed against membrane thickness (Table 2) for each of the blend conditions: strength, secant stiffness, toughness and ductility (Figure 5). The strongest membranes are those made from the high-molecular-weight A, while the weakest membranes are those made from the low-molecular-weight B. As expected, the three blends fall between 100% A and 100% B relatively in

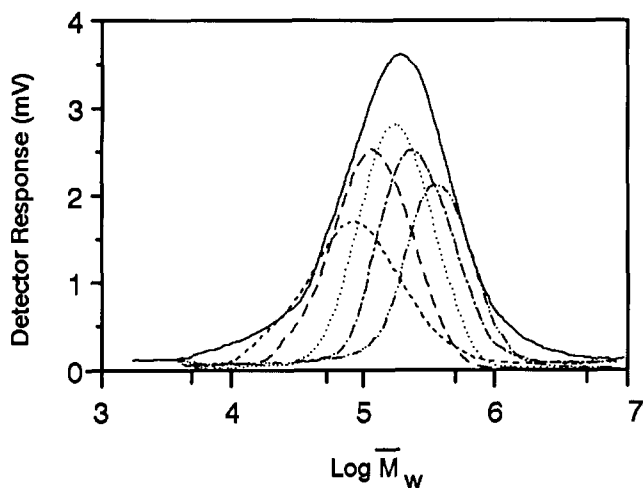


Figure 4 G.p.c. chromatogram showing the relative distribution of the fractionated polymers and its whole polymer: OXY 410 (—), F1 (---), F2 (·····), F3 (— · — ·), F4 (— · — ·), F5 (-----)

order. Membrane strength, as well as secant stiffness and toughness, increases with membrane thickness. Secant stiffness and toughness show similar sample ranking with respect to blend condition as seen in the strength results. Membrane ductility appears to be independent of membrane thickness.

Failure parameters for fractionated PVC blends show that the strongest membranes are made from the high-molecular-weight F2 and the weakest membranes from the low-molecular-weight F5 (Figure 6). Once again the intermediate blends rank according to their molecular weights. Toughness and – to a lesser extent – secant stiffness show a similar rank ordering. Ductility again shows no relation to membrane thickness, as the regression slopes vary about zero (Table 3).

Of all membranes tested, those made from F2 exhibited the highest strengths and toughnesses; the weakest membranes were made from B, and the least tough were made from F5. Secant stiffnesses of membranes made

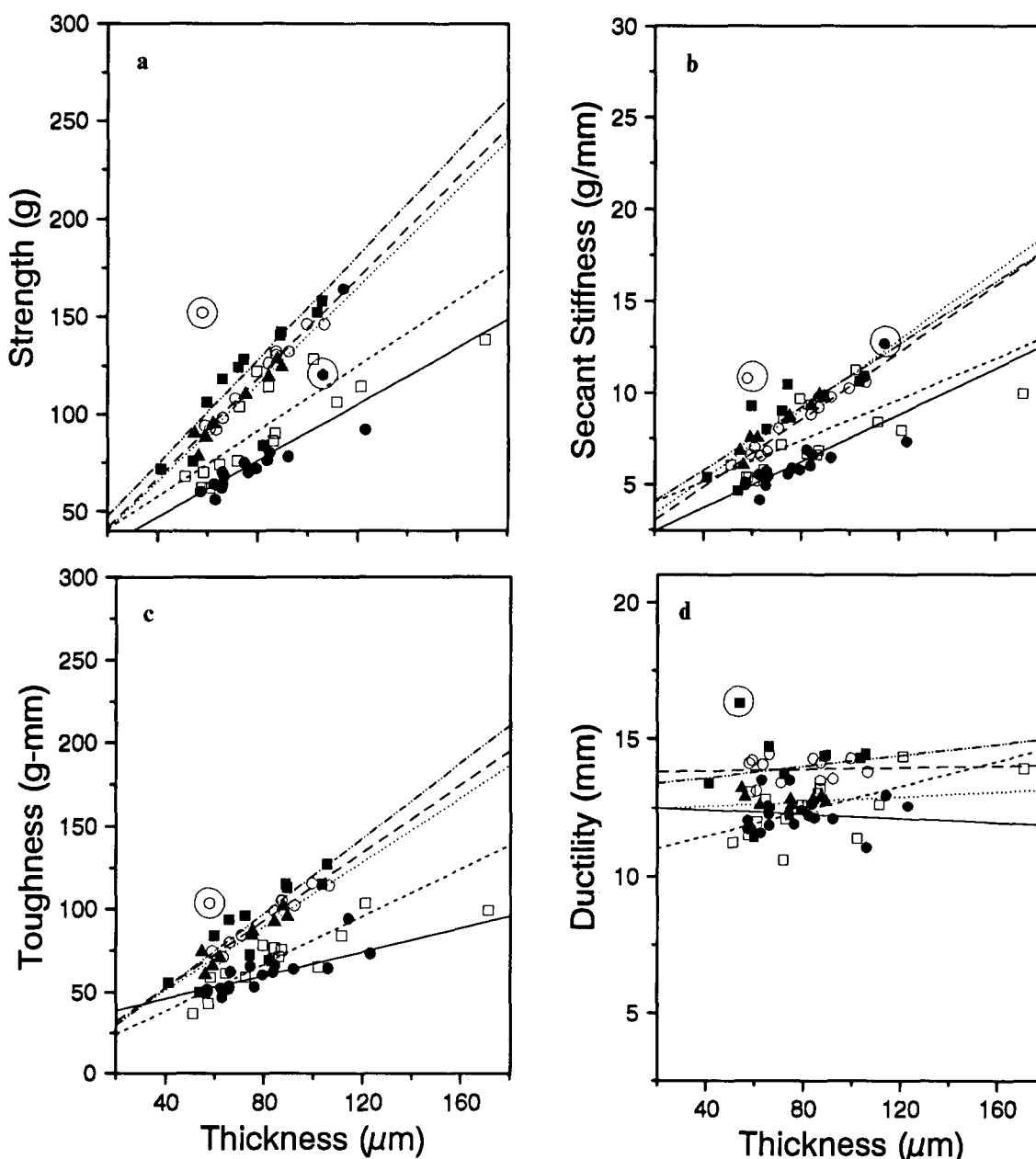
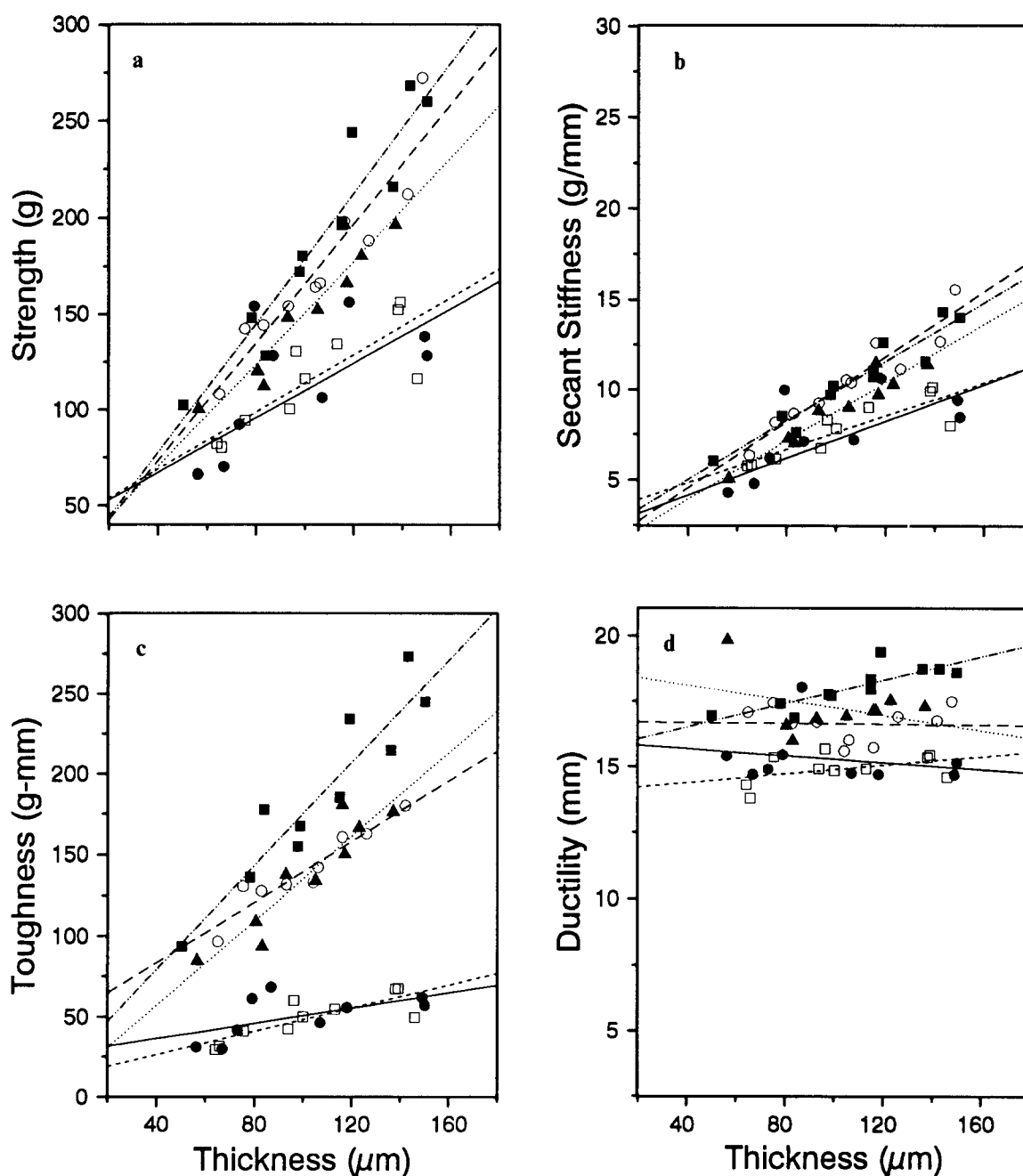


Figure 5 Failure parameters (cf. Figure 2) of whole blends as a function of membrane thickness: 100% A (■, — · — ·), 75% A/25% B (○, — —), 50% A/50% B (▲, ·····), 25% A/75% B (□, - - - -) and 100% B (●, —). Corresponding slopes ( $m$ ) and probabilities ( $p$ ) are detailed in Table 2

**Table 2** Regression slopes ( $m$ ) of mechanical properties for whole blends *versus* thickness

Blend	$n$	Failure				Elastic			
		Strength (g)	Secant stiffness ( $\text{g mm}^{-1}$ )	Toughness (g mm)	Ductility (mm)	Elastic limit (g)	Tangent stiffness ( $\text{g mm}^{-1}$ )	Resilience (g mm)	Flexibility (mm)
100% B	17	0.72*	0.063*	0.48*	-0.004***	0.54*	0.13*	0.15*	0.009***
25% A/75% B	15	0.84*	0.056**	0.71*	0.022***	0.56*	0.15*	0.14***	0.018***
50% A/50% B	9	1.24*	0.094*	0.97*	0.004***	0.99*	0.19*	0.31*	0.009***
75% A/25% B	11	1.28*	0.091*	1.02*	0.001***	0.89*	0.18*	0.28*	0.013***
100% A	10	1.34*	0.085*	1.13*	0.010***	0.69*	0.13**	0.22**	0.005***

\*Significant at  $p < 0.001$ . \*\*Significant at  $p < 0.01$ . \*\*\*Not significant ( $p > 0.05$ )



**Figure 6** Failure parameters (cf. Figure 2) of fractionated blends as a function of membrane thickness: 100% F2 (■, — · — ·), 75% F2/25% F5 (○, — — —), 50% F2/50% F5 (▲, ·····), 25% F2/75% F5 (□, - - - -) and 100% F5 (●, — — —). Corresponding slopes ( $m$ ) and probabilities ( $p$ ) are detailed in Table 3

Table 3 Regression slopes (*m*) of mechanical properties for fractionated blends versus thickness

Blend	<i>n</i>	Failure				Elastic			
		Strength (g)	Secant stiffness (g mm <sup>-1</sup> )	Toughness (g mm)	Ductility (mm)	Elastic limit (g)	Tangent stiffness (g mm <sup>-1</sup> )	Resilience (g mm)	Flexibility (mm)
100% F5	8	0.72	0.051**	0.24**	-0.007***	0.58**	0.11*	0.11**	0.006***
25% F2/75% F5	10	0.75**	0.046**	0.36	0.008***	0.65**	0.10**	0.13**	0.008***
50% F2/50% F5	9	1.34*	0.081*	1.30*	-0.014***	0.75*	0.13*	0.16*	0.023***
75% F2/25% F5	10	1.55*	0.091*	0.93*	-0.001***	0.71*	0.16*	0.10*	-0.004***
100% F2	11	1.69*	0.082*	1.60*	0.022**	0.74*	0.14*	0.12**	0.010***

\*Significant at  $p < 0.001$ . \*\*Significant at  $p < 0.01$ . \*\*\*Not significant ( $p > 0.05$ )

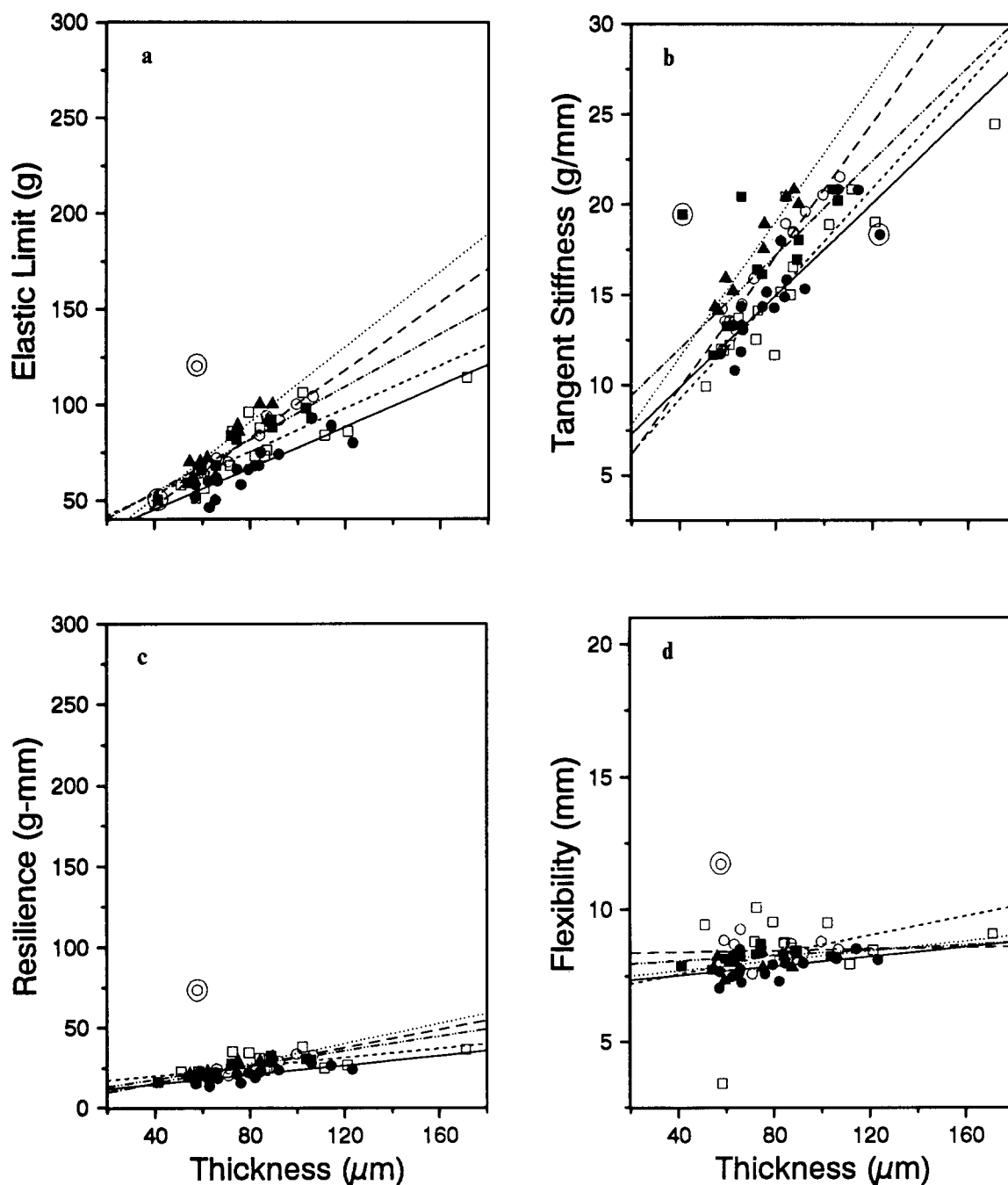


Figure 7 Elastic parameters (cf. Figure 3) of whole blends as a function of membrane thickness (see Figure 5 for details)

from fractionated polymers, whole polymers and their blends overlap each other nearly exactly. Ductilities of membranes made from fractionated polymers and their blends are in general higher and more disperse than those made from whole polymers.

**Elastic parameters.** All elastic parameters are displayed using the same scales as the failure parameters. Membranes that were made from whole blends (Figure 7) exhibit increasing elastic limits with increasing thicknesses (Table 2). The 50% A/50% B blend showed the highest elastic limit, followed by the 75% A/25% B blend and the 100% A; the 100% B showed the lowest elastic limit. Tangent stiffness and resilience both showed the same rank ordering as the elastic limit data, i.e. 50% A/50% B is the most resilient and has the highest tangent stiffness, while 100% B is the least resilient and

has the lowest tangent stiffness. Flexibility was unaffected by membrane thickness.

Elastic parameters of membranes that were made from fractionated blends (Figure 8) show positive slopes when elastic limits, tangent stiffnesses and resiliences are regressed against thicknesses (Table 3). Flexibility was once more independent of membrane thickness. The highest elastic limits belonged to 75% F2/25% F5 membranes with 50% F2/50% F5 and 100% F2 membranes close behind (cf. Figure 8). The lowest was 100% F5. All membranes had similar resiliences that showed only a slight effect of membrane thickness. Tangent stiffness had the same rank ordering as the elastic limit data.

The membranes made from fractionated polymers and their blends had elastic limits within the range prescribed by the whole polymer elastic limits. The resiliences of

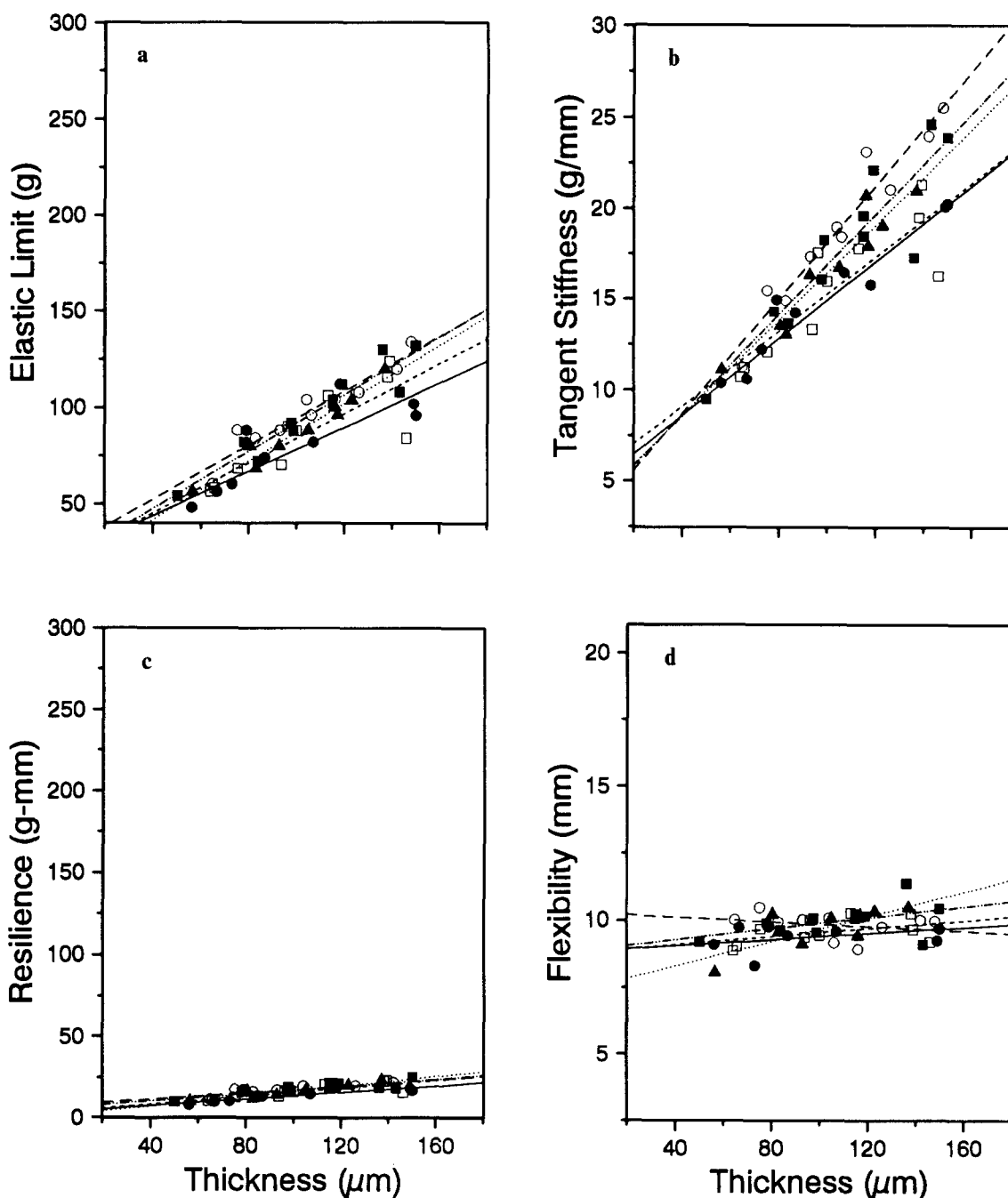


Figure 8 Elastic parameters (cf. Figure 3) of fractionated blends as a function of membrane thickness (see Figure 6 for details)



membranes made from whole polymers and their blends were higher than those made from fractionated membranes, yet all membranes showed little thickness dependence. Membranes made from 50% A/50% B and 75% A/25% B had the highest tangent stiffnesses of all membranes. Flexibility was highest for membranes made from fractionated polymers and their blends.

#### Statistics

Three outlying points were discovered in the data set of whole blends (total samples = 65), one each in the 100% A, 100% B and 75% A/25% B (cf. Figures 5 and 7). No outlying points were found in the data set of fractionated blends (total samples = 48) (cf. Figures 6 and 8).

## DISCUSSION

### Biosensor design

A critical condition for proper ISE functioning is that the electrode membrane remain intact. ISE failure has been shown to be caused primarily by membrane rupture<sup>21</sup>. Even in these membranes with 200 phr DOS, the mechanical properties are determined by the minor component, PVC (cf. Figures 5–8). In terms of conventional plasticized polymer systems, these membranes essentially represent a reverse-phase system – where the plasticizer is the matrix, and the polymer is the dispersed phase. Since the polymer still provides the structural support for these membranes, a mechanically sound design must principally include the polymer, given its unique role in these ISEs.

### Mechanical properties

The mechanical properties of fractionated and whole blends are not substantially different. Therefore fractionation, which affords the advantage of greater cleanliness and purity, does not detract from the mechanical performance of the polymer, when incorporated into ISE membranes.

*Failure parameters.* The mechanical properties of strength and toughness are highly affected by membrane thickness (cf. Figures 5 and 6). The regression slopes for these parameters often equal about 1.0 and are highly significant (cf. Tables 2 and 3). Secant stiffness slopes range in value from 0.05 to 0.09 (cf. Tables 2 and 3), indicating a weaker thickness effect. Ductility is independent of membrane thickness, as the slopes approach zero, accounting for the poor regression correlation coefficients observed (cf. Tables 2 and 3).

*Elastic parameters.* In the elastic region, the mechanical properties of membranes are more uniform than in the plastic region. The range of the elastic parameter data varies less than the failure parameter data. As expected, elastic parameters have lower values than their failure analogues – with the exception of tangent stiffness. Tangent stiffness corresponds to the first sharp upward swing of the force–deflection trace; its values should be and are higher than those of secant stiffness (cf. Figures 5 vs. 7 and Figures 6 vs. 8). The slopes of both elastic limit and resilience versus thickness are less steep than they were for the analogous failure parameters of strength and toughness (cf. Tables 2 and 3) and indicate a

diminished effect of membrane thickness. As was the case for ductility, the flexibility is independent of membrane thickness (cf. Tables 2 and 3).

### Independence of deflection parameters on thickness

The flexibility and ductility of a membrane appears to be dependent on the intermolecular bonding of the individual PVC molecules and entanglements rather than membrane thickness. Large negatively charged chlorine atoms on alternate carbons of the polymer backbone serve to stiffen the main chain by steric hindrance and electron repulsion, while providing molecular attraction between adjacent chains. Entanglements are possible because the molecular weights of all polymers and blends used (cf. Table 1) are greater than the entanglement molecular weight of about 10 000 for PVC, albeit the membranes are highly plasticized.

The method of testing is essentially biaxial; that is, the membranes are deformed by the probe and stretched in tension parallel to the casting plane. The initial shape of each force–deflection trace indicates that a substantial non-linear elastic zone exists (e.g. Figure 3a) in which flexibility is independent of thickness. Succeeding this zone, plastic deformation via molecular realignment occurs. This realignment is quite facile, because the PVC molecules reside in such a highly plasticized solution that the glass transition temperature is far below room temperature, thereby promoting short relaxation times. Upon further displacement of the membrane, a plateau region is established in the plastic zone (Figure 3a), which represents the attainment of a critical resolved force that continues the realignment process until a limiting, if not optimal, orientation is achieved. At that juncture, the force resisting the probe then increases rapidly to failure as molecules slip and cracks develop (Figure 3a).

As a consequence of this deformation and alignment, an anisotropic structure develops in which the tensile strength normal to the axes of the molecular orientation will be less than that parallel to the casting plane, since only secondary (intermolecular) bonds and entanglements predominate rather than primary (intramolecular) bonds. Thus, the plane of failure is in the thickness direction. As chains reorient during force application, the ends of neighbouring chains come into close proximity, eliminating any secondary bonding possible at that location and thereby inducing a flaw. If this flaw is of critical length, a crack is nucleated and grows in the thickness direction as an outcome of this stress concentration. A nucleated crack, with a dimension much less than the thickness of the membrane, will bring about failure soon thereafter.

Ultimately, the initiation of a flaw and the subsequent nucleation of a crack are the key processes in these highly plasticized PVC membranes, since they contain only one-third as many molecules as a minimally plasticized membrane to resist the propagation of an induced crack. Ductility measurements are independent of thicknesses because crack nucleation, and not crack propagation, is the limiting process. Flexibility magnitudes are restricted by the extent to which chains can elastically orient; whereas, ductility magnitudes are restricted by the extent to which chains can plastically orient, bonds can stretch and flaws can nucleate into cracks.

### Polymer blending

Work done in the late 1940s by Fox and Flory<sup>22–24</sup> established that mixtures of different polymer compositions

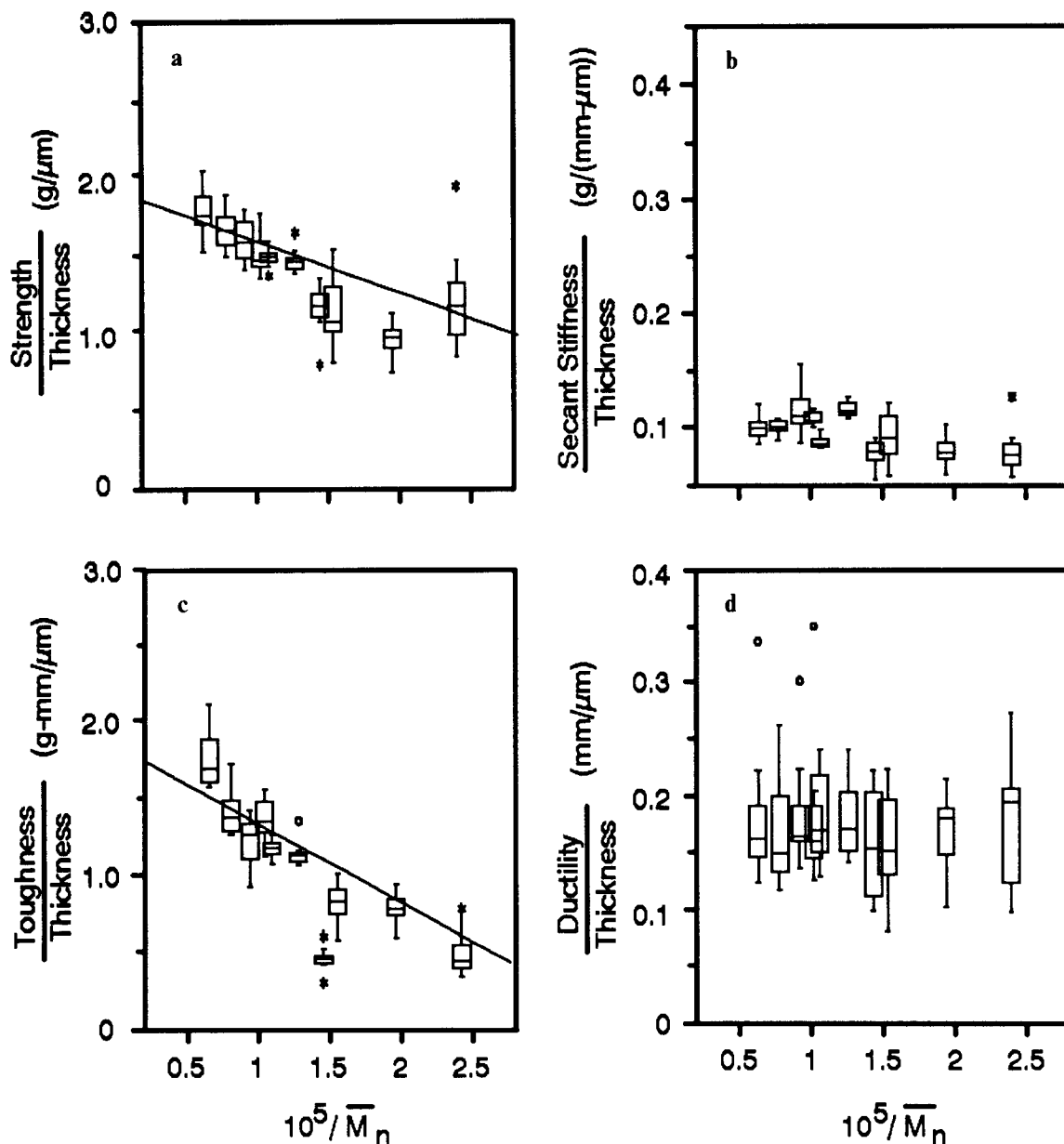


**Figure 9** Box plots of failure parameters for both whole and fractionated polymer blends versus the calculated blend  $\bar{M}_n^{-1}$ . See footnote in text for interpretation of a box plot

could be treated as the arithmetic average of their component chain lengths in the same way that a summation of  $\bar{M}_n$  representing consecutive slices of the molecular-weight distribution would be used to calculate the  $\bar{M}_n$  of a whole polymer<sup>25</sup>. In this study, a relatively high- $\bar{M}_w$  PVC was blended with a low- $\bar{M}_w$  PVC. The effective  $\bar{M}_n$  values of each blend were calculated by estimating the volume fractions of the PVCs in each blend.

All mechanical parameters were first normalized by thickness and then graphed in box plot form<sup>26</sup> against the inverse of the effective  $\bar{M}_n$  multiplied by  $10^5$  (Figures 9 and 10).<sup>\*</sup> The data from all the blends are consolidated

<sup>\*</sup> Each box contains the first and third quartiles of the data (interquartile range or *IQR*) encompassing 50% of the data, and includes the median, as indicated by a line across the box. Data outside the box, but within 1.5 times the *IQR*, are expressed as whiskers that extend above and below the box. Mild outliers (within 1.5 to 3 times the *IQR*) are shown by asterisks, and extreme outliers (greater than 3 times the *IQR*) are illustrated by open circles

on one plot for each mechanical parameter. When the averages of the mechanical parameters were regressed against the inverse of  $\bar{M}_n$  (Table 4), the elastic parameters are independent of polymer chain length (Figure 10), as all regression slopes are near zero and no significant correlations exist. These processes should be molecular-weight-independent, since the chain motion in this region of the force-deflection trace mainly involves recoverable stretching of the intermolecular bonds. Such local motion takes place in the elastic region<sup>27</sup>. One failure parameter (Figure 9) definitely shows no effect of polymer chain length, ductility/thickness; as discussed earlier, it is determined only by individual molecule-to-molecule interactions and is therefore independent of the number of molecules or  $\bar{M}_n$ . Secant stiffness/thickness, while not significant at  $p < 0.01$ , does show a slight effect of  $\bar{M}_n$ . Secant stiffness is determined essentially by the quotient of strength and ductility (cf. Figure 2). As ductility varies widely within a given  $\bar{M}_n$ , its effect in the secant stiffness calculation would be to decrease the

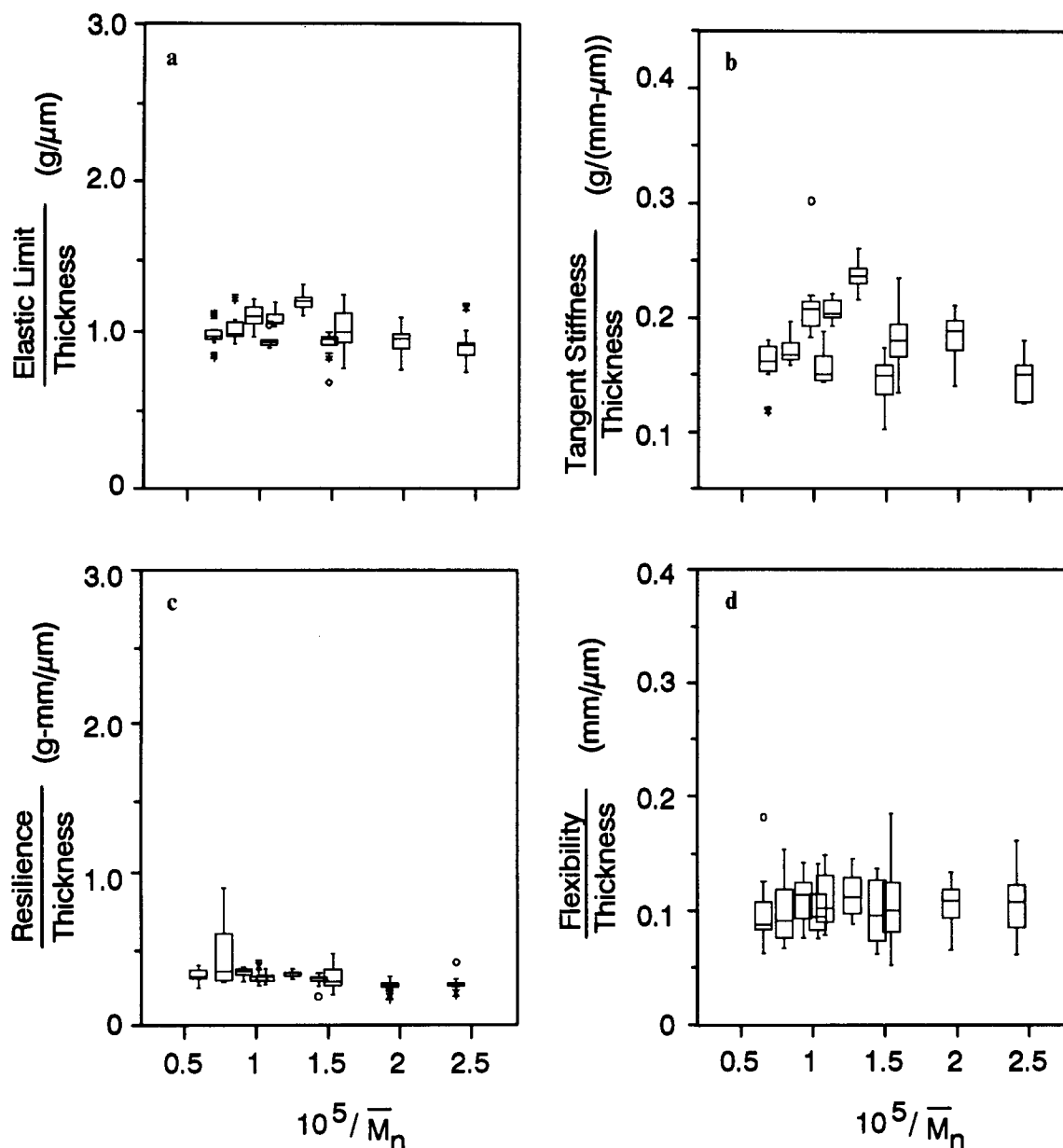


Figure 10 Box plots of elastic parameters for both whole and fractionated polymer blends versus the calculated blend  $\bar{M}_n^{-1}$ . See footnote in text for interpretation of a box plot

Table 4 Regression results of mechanical properties versus blend  $\bar{M}_n^{-1}$

Biometrics	Failure				Elastic			
	Strength (g)	Secant stiffness (g mm <sup>-1</sup> )	Toughness (g mm)	Ductility (mm)	Elastic limit (g)	Tangent stiffness (g mm <sup>-1</sup> )	Resilience (g mm)	Flexibility (mm)
<i>n</i>	10	10	10	10	10	10	10	10
<i>r</i>	0.84	0.63	0.84	0.40	0.43	0.24	0.63	0.20
<i>m</i>	-0.41**	-0.017***	-0.62**	-0.008***	-0.08***	-0.01***	-0.06***	0.002***
<i>y</i> intercept	1.95	0.119	1.86	0.185	1.06	0.21	0.42	0.103

\*Significant at  $p < 0.001$ . \*\*Significant at  $p < 0.01$ . \*\*\*Not significant ( $p > 0.05$ )

significance of any measured slope. Among the four failure parameters, however, chain length appears as an important predictor in two cases – that of strength/thickness and toughness/thickness.

If failure can be assumed to originate in some way at the ends of the molecules (e.g. cf. ref. 28), then the strength

and toughness must depend on the number of polymer chain ends, hence  $\bar{M}_n$ . Longer polymer chains limit the possible origins of failure. Additionally, the numbers of intermolecular bonds and entanglements, which are the primary determinants of strength and toughness, increase with polymer chain length. In earlier work on the

stress-strain behaviour of polymers, other researchers have found a relationship between  $\bar{M}_n$  and polymer properties<sup>29-32</sup>. In other work, it was shown that a combination of  $\bar{M}_n$  and  $\bar{M}_w$  was required to account for the tensile strength of rigid polystyrene<sup>33</sup>. Nonetheless, the equation most often applied for predicting the tensile strength of blends of fractions is:

$$\sigma = \sigma_0 - (K/\bar{M}_n) \quad (1)$$

in which  $\sigma_0$  is the tensile strength at a limiting high molecular weight of polymer, and  $K$  is an empirical constant<sup>34</sup>. This form of the equation has been applied to many mechanical and material properties: tensile strength, modulus and elongation<sup>24,25,35,36</sup>. In the current membranes, by regressing the average mechanical property values (cf. *Figures 9* and *10*) against the reciprocal  $\bar{M}_n$  values of the blends, the failure parameters of strength/thickness and toughness/thickness can be related to molecular chain length as:

$$\frac{\text{Strength (g)}}{\text{Thickness } (\mu\text{m})} = 1.95 - \frac{4.14 \times 10^4}{\bar{M}_n} \quad (2)$$

and

$$\frac{\text{Toughness (g mm)}}{\text{Thickness } (\mu\text{m})} = 1.86 - \frac{6.19 \times 10^4}{\bar{M}_n} \quad (3)$$

These relationships suggest that a specific strength and toughness can be attributed to each length of polymer chain and further to each mer of PVC in a 200 phr membrane plasticized with DOS. A polymer sample with  $\bar{M}_n = 100\,000$  contains roughly 1600 mers (assuming a mer molecular weight of  $62.5 \text{ g mol}^{-1}$ ). The strength per micrometre thickness according to equation (2) for such a sample is  $1.5 \text{ g } \mu\text{m}^{-1}$ . This results in a contribution of  $0.96 \text{ mg } \mu\text{m}^{-1}$  from each mer. Similar calculations for toughness conclude that each mer contributes  $0.78 \text{ mg mm } \mu\text{m}^{-1}$ . The equations also indicate a limiting strength/thickness value of  $2.0 \text{ g } \mu\text{m}^{-1}$  and a limiting toughness/thickness value of  $1.9 \text{ g mm } \mu\text{m}^{-1}$ . Eventually, the trends depicted in *Figures 9a* and *9c* would approach these limiting values at very high  $\bar{M}_n$  values.

## CONCLUSIONS

Membranes made from fractionated PVC plasticized at a level of 200 phr do not show substantially different mechanical properties than those made from whole PVC similarly plasticized.

Membrane properties in the elastic region are not affected by polymer  $\bar{M}_n$ .

Membrane ductility is independent of thickness, as it is determined only by the conformation of the polymer chains in the casting plane.

By applying a linear blending relationship for  $\bar{M}_n$ , chain length becomes an important predictor for two mechanical properties at failure: strength/thickness and toughness/thickness. These relationships indicate an individual PVC mer contribution of  $0.96 \text{ mg } \mu\text{m}^{-1}$  for

strength/thickness and  $0.78 \text{ mg mm } \mu\text{m}^{-1}$  for toughness/thickness.

## ACKNOWLEDGEMENT

The authors are grateful to the following for funding: National Science Foundation/Engineering Research Center (NSF/ERC) and Center for Emerging Cardiovascular Technologies, Duke University, Durham, NC.

## REFERENCES

- 1 Thomas, J. D. R. *Anal. Chim. Acta* 1986, **180**, 289
- 2 Tuczai, E. and Cortolano, F. *Mod. Plast.* 1992, **69**, 123
- 3 Ghersa, P. *Mol. Plast.* 1958, **36**(2), 135 and 212
- 4 Siggia, S. and Hark, H. F. in 'Polymer Science and Materials' (Eds A. V. Tobolsky and H. F. Mark), Wiley-Interscience, New York, 1971, p. 37
- 5 Park, J. 'Biomaterials', Plenum Press, New York, 1979, pp. 82-5
- 6 Sperling, L. H. 'Interpenetrating Polymer Networks and Related Materials', Plenum Press, New York, 1981, pp. 26-28
- 7 Kryszewski, M. in 'Polymer Blends' (Eds E. Martuscelie, R. Palumbo and M. Kryszewski), Plenum Press, New York, 1980, pp. 1-22
- 8 Ghaffar, A., Scott, G. and Crowther, P. *Eur. Polym. J.* 1978, **14**, 631
- 9 Pakula, T. in 'Polymer Blends' (Eds E. Martuscelie, R. Palumbo and M. Kryszewski), Plenum Press, New York, 1980, pp. 239-264
- 10 Ueda, H., Karasz, F. E. and Farris, R. S. *Polym. Eng. Sci.* 1986, **26**, 1483
- 11 Moody, G. J. and Thomas, J. D. R. 'Ion-Selective Microelectrodes', Springer-Verlag, Berlin, 1986, pp. 55 and 88
- 12 Oesch, U. and Simon, W. *Anal. Chem.* 1980, **52**, 692
- 13 Ammann, D. 'Ion-Selective Microelectrodes'. Springer-Verlag, Berlin, 1986, p. 88
- 14 Brandrup, J. and Immergut, E. H. (Eds) 'Polymer Handbook', 2nd Edn, Wiley, New York, 1975, p. IV-14
- 15 Chartoff, R. P. and Lo, S. K. T. in 'Liquid Chromatography of Polymers and Related Materials' (Ed. J. Cazes), Marcel Dekker, New York, 1977, Vol. 8, pp. 135-148
- 16 Abdel-Alim, A. H. and Hamielec, A. E. *J. Appl. Polym. Sci.* 1973, **17**, 3033
- 17 Craggs, A., Moody, G. J. and Thomas, J. D. R. *J. Chem. Educ.* 1970, **15**, 541
- 18 Peng, T., Kusy, R. P., Garner, S. C., Hirsch, P. F. and DeBlanco, M. C. *J. Bone Mineral Res.* 1987, **2**, 249
- 19 Ortolani, S. and Trevisan, C. *Bone and Mineral* 1993, **22** (Suppl.), S7-S22
- 20 Simon, M. A. and Kusy, R. P. *Polymer* 1993, **34**, 5106
- 21 Kusy, R. P. and Buchanan, J. W. *Microbeam Anal.* 1989, 63
- 22 Fox, T. G. and Flory, P. J. *J. Am. Chem. Soc.* 1948, **70**, 2384
- 23 Fox, T. G. and Flory, P. J. *J. Appl. Phys.* 1950, **21**, 581
- 24 Flory, P. J. *Ind. Eng. Chem.* 1946, **38**, 417
- 25 Callister, W. D. 'Materials Science and Engineering: An Introduction', 2nd Edn, Wiley, New York, 1991, p. 466
- 26 Simpson, R. J., Johnson, T. A. and Amara, I. A. *Am. Heart J.* 1988, **116**, 1663
- 27 Kramer, O. *Br. Polym. J.* 1985, **17**, 129
- 28 Peterlin, A. *J. Macromol. Sci.-Phys. (B)* 1973, **8**, 83
- 29 Sookne, A. M. and Harris, M. *J. Res. Nat. Bur. Stand.* 1943, **30**, 1
- 30 Sookne, A. M. and Harris, M. *Ind. Eng. Chem.* 1945, **37**, 478
- 31 Mandelkern, L., McLaughlin, K. W. and Alamo, R. G. *Macromolecules* 1992, **25**, 1440
- 32 Flory, P. J. *J. Am. Chem. Soc.* 1945, **67**, 2048
- 33 Merz, E. H., Nielsen, L. E. and Buchdahl, R. *Ind. Eng. Chem.* 1951, **43**, 1396
- 34 Nielsen, L. E. 'Mechanical Properties of Polymers and Composites', Marcel Dekker, New York, 1974, Vol. 2, p. 273
- 35 Jacobi, H. R. *Kunststoff* 1953, **43**, 9
- 36 Vincent, P. I. *Polymer* 1960, **1**, 425